Received: 3 July 2020 | Revised: 6 October 2020 | Accepted: 20 November 2020

DOI: 10.1002/pip.3383

RESEARCH ARTICLE

PROGRESS IN PHOTOVOLTAICS WILEY

Recover possibilities of potential induced degradation caused by the micro-cracked locations in p-type crystalline silicon solar cells

Dong C. Nguyen[1,2] | Yasuaki Ishikawa[1,3] | Yukiharu Uraoka[1]

[1]Division of Materials Science, Nara Institute of Science and Technology, Ikoma, Nara, Japan

[2]Institute of Research and Development, Duy Tan University, Danang, 550000, Vietnam

[3]College of Science and Engineering, Aoyama Gakuin University, Sagamihara, Kanagawa, Japan

Correspondence
Yasuaki Ishikawa, College of Science and Engineering, Aoyama Gakuin University, Sagamihara, Kanagawa, Japan.
Email: yishikawa@ee.aoyama.ac.jp

Abstract

Potential induced degradation (PID) has been affecting the performance, durability, and reliability of crystalline Si solar cells/modules. The authors demonstrate that micro-cracks also act as the additional recombination centers, which reduce short-circuit current density (J_{sc}), open-circuit voltage (V_{oc}), and the effective lifetime of carriers in solar cells, in PID condition. This hypothesis was confirmed by external quantum efficiency measurements and microwave photo-conductance decay method at the micro-cracked areas before and after PID stress tests. In addition, the PID recovery was made significantly but non-fully for the laminated micro-cracked modules owing to the electrical PID recovery method. In addition, the authors showed and discussed the challenging problems in recovering the performance of the PID-affected micro-cracked solar modules without lamination. The achieved results from 11 cycles of PID stress/recovery tests with the same duration of PID stress and recovery processes showed that an exponentially decreasing function fits the correlation between the relative losses of P_{max}, V_{oc}, fill factor (FF), and J_{sc} due to the PID stress process and the number of the PID stress/recovery cycles. This provides a model for the estimation of the relative losses of P_{max}, V_{oc}, FF, and J_{sc} due to the PID stress process versus the number of the PID stress/recovery cycles. Finally, based on the decreasing tendency in the performance loss of the PID-affected laminated micro-cracked solar modules after PID stress/recovery cycles, the authors suggest that cyclic PID tests with suitable conditions might be a reasonable approach to control PID.

KEYWORDS

cyclic PID test, exponential model, micro-crack, PID recovery, potential induced degradation (PID)

1 | INTRODUCTION

The term of potential induced degradation (PID) was firstly introduced in 2010 as one of the degradation types for solar cells by Pingel et al.[1] and other works.[2,3] The appearance of PID in solar cells causes the degradation of performance, durability, reliability, and even the destruction of the solar cells. A high potential difference between the aluminum frames and the solar cells induced in standard photovoltaic (PV) systems under working conditions could lead to significant yield losses after a long time of use if the solar cells are prone to PID. PID shunting (PID-s) is the primary mechanism in standard p-type crystalline silicon (c-Si) solar cells,[1,2,4] and PID polarization (PID-p) is the important mechanism in n-type c-Si solar cells.[5–7] The PID-s defects occur when Na ions enter and decorate in stacking faults[8] and

micro-cracks[9] of solar cells. The feature of PID-s defects is the severe reduction of shunt resistance (R_{sh}), leading to the degradation of the performance and lifetime of the solar cells.

It is well known that cracks with their width below 100 μm are considered micro-cracks.[10] Although the size of micro-cracks in solar cells is too small to be seen by the naked eye, they still degrade the performance and reliability of solar cells. The influence level of micro-cracks on the degradation depends on the length, width, depth, and type of micro-cracks. The micro-crack induced deterioration becomes more severe after the aging process by humidity freeze cycles.[11,12] In particular, the electric characteristics of solar cells have severely deteriorated where the PID phenomenon has been observed in micro-cracked areas of p-type crystalline silicon solar cells. The cause of the PID effect in micro-cracked regions is related to the decoration of the Na ions investigated.[13] However, there is no research to overcome the performance deterioration owing to the PID effect related to micro-cracks. Therefore, a PID recovery process should be examined for the PID-affected micro-cracked solar cells.

A PID recovery method by biasing a reversed voltage for PID-affected micro-cracked p-type c-Si solar cells with and without lamination was utilized in this work. PID stress/recovery cycles were also performed for micro-cracked solar cells. The electrical characteristics of the solar cells were measured and analyzed before and after PID stress and recovery processes. Furthermore, characterizations composed of electroluminescence (EL), lock-in thermography (LIT) images, dark and illumination current density-voltage (*J-V*) curves, external quantum efficiency (EQE) responses, and effective carrier's lifetime (τ_{eff}) were utilized to support analyses and conclusions of this work.

2 | EXPERIMENTAL PROCEDURE

2.1 | PID stress and recovery processes of solar modules

Two commercial p-type based c-Si solar cells with large size of 156 mm × 156 mm and a thickness of 200 μm were utilized in this work. The first large cell was cut into small pieces with a size of 15 mm × 15 mm by a micromachining system (Oxford Lasers Ltd.). Six similar small pieces called mini-cells were employed in this work as well. Three mini-cells had micro-cracks induced by the mechanical method, and the rest of the mini-cells were kept intact. Because the accuracy of using a shadow mask to measure local *J-V* characteristics in micro-cracked and intact regions of a large solar cell is restricted, mini micro-cracked and intact solar cells need the experiments to ensure the more precise measurement of the photo *J-V* curves without the shadow mask. As shown in Figure 1a, the structure of a mini solar module consists of one mini-cell between two commercial first-cure type ethylene-vinyl acetate (EVA) films, one soda-lime glass plate on the top of EVA film, and one backsheet below the bottom EVA film. The thickness of the EVA film and glass plate are 450 μm and 3.2 mm, respectively. The EVA film, the glass, and the backsheet have a size of 60 mm × 60 mm. The backsheet is composed of polyvinyl fluoride (PVF) of 38 μm/polyethylene terephthalate (PET) of 250 μm/PVF of 38 μm. It is noted that six mini solar modules, which were laminated by heating and load (lamination process) for 1 h before all experimental tests, as illustrated in Figure 1b, are called laminated solar modules.

On the other hand, we formed several micro-cracked areas in the other large cell by the same mechanical method and made one large module from the micro-cracked large cell. The structure of the large module is composed of one large micro-cracked cell located between two EVA films and two soda-lime glasses with a size of 200 mm × 200 mm covering both top and bottom EVA films. However, the micro-cracked large module, which was not laminated during the experimental processes, is called the un-laminated solar module. Such a structure of un-laminated solar modules was examined and utilized for both PID stress and recovery tests in the works of Lausch et al.[14,15] This is to easily separate the active solar cell from the EVA films for the analysis of other microstructural characteristics in PID-affected solar cells.[13]

A PID stress test of solar modules was carried out in a climatic chamber (LH-113, Espec Co.), as illustrated in Figure 1a. Herein, an aluminum (Al) foil acts as the grounded frame of a solar module. The

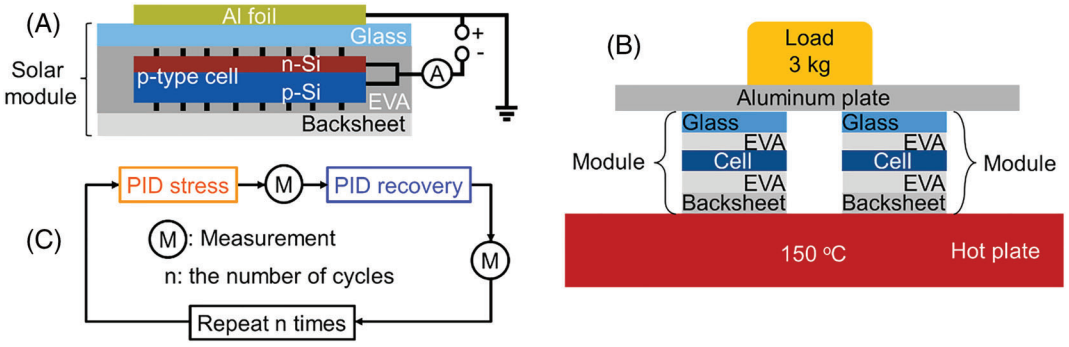

FIGURE 1 (A) The diagram of the PID stress setup, (B) the diagram of a laminating process, and (C) the flow chart of the PID stress/recovery cycles

negative and positive terminals of the high voltage power source (PID insulation Tester, TOS7210S, Kikusui Electronics Co.) are connected to the two shortened leads and the grounded frame of a solar module, respectively. The laminated modules were subjected to PID stress tests with a duration of up to 96 h under a high negative voltage of −1,000 V, a temperature of 85°C, and a relative humidity (RH) of 85%. Meanwhile, the un-laminated module was subjected to a PID stress test with a duration of 150 h under a high negative voltage of −1,000 V, a temperature of 65°C (<85°C to avoid the melting of EVA films), and RH of 85%. PID recovery tests were performed by biasing a high positive voltage of +1,000 V (reverse voltage) between a solar cell and the Al foil under the same RH of 85% and temperature of 85°C with a recovery duration up to 96 h.

In this study, the cyclic PID stress/recovery tests with the same duration of 72 h for stress and recovery were also performed in 11 cycles for laminated micro-cracked solar modules, as shown in Figure 1c. The first step is to conduct the PID stress process (−1,000 V, 85°C, 85% RH) for the laminated micro-cracked solar modules. After necessary measurements, the second step is to proceed the PID recovery process (+1,000 V, 85°C, 85% RH) for the PID-affected solar modules of the first step. Also after measurements, the PID stress and recovery processes were repeated 11 times (cycles). It is noted that measurements were conducted immediately after cooling down the solar modules to room temperature (25°C).

2.2 | The measurement of electrical characteristics of solar modules

EL and LIT images were taken by a THEMOS-1100L (Hamamatsu Photonics K. K.) with the InGaAs camera cooled at around −70°C for the laminated and un-laminated solar modules before and after the PID stress and recovery processes with the applied current density of 10 mA/cm^2. Dark current-voltage (*I-V*) and illumination *J-V* curve characteristics of solar modules were measured by a solar simulator under an AM 1.5 irradiance spectrum (1 sun, 25°C). EQE responses were characterized by a CEP-2000RP (Bunkokeiki Co., Ltd.). Notably, to get acceptable measured results at local areas of the un-laminated micro-cracked solar module, measurements of the illumination *J-V* characteristics and EQE responses at the micro-cracked region were made by using a shadow mask with a slot of 15 mm × 15 mm in size.[13] Meanwhile, measurements of the illumination *J-V* characteristics and EQE responses were characterized in the whole area of laminated micro-cracked and intact solar modules without the shadow mask. Electrical characteristics of solar cells, including P_{max}, V_{oc}, FF, and J_{sc}, were extracted from the above one-sun illumination *J-V* curves. The value of R_{sh} and R_s was estimated according to the equivalent circuit of the double diode model for the slope of the light *J-V* curve at $V = 0$ and $V = V_{oc}$ through Equations 1 and 2.[16,17]

$$R_{sh} = \left| \left(\frac{dI}{dV} \right)^{-1}_{V=0} \right| \quad (1)$$

$$R_s = \left| \left(\frac{dI}{dV} \right)^{-1}_{V=V_{oc}} \right| \quad (2)$$

The microwave photo-conductance decay (μ-PCD) signal curves and τ_{eff} values of solar cells were directly measured by a commercially available μ-PCD measurement system (WT-1000B, Semilab Inc.) with an applied laser wavelength of 904 nm. The μ-PCD measurement system could be used as a method that indicates the PID behavior of c-Si solar cells, as reported in some publications.[9,18]

3 | RESULTS AND DISCUSSION

3.1 | The behavior of PID stress and recovery in micro-cracked un-laminated solar modules

Figure 2 showed EL and LIT images of the micro-cracked un-laminated solar module before and after the PID stress for 150 h and after the PID recovery for 75 h and 150 h. The micro-cracked un-laminated solar module is subjected to PID stress for 50 h and 100 h had been reported in our previous work.[13] In this work, the PID-shunting defect extending at around the micro-cracked areas after PID duration of 150 h was also observed in the dark regions of EL images as well as the corresponding hot spots in LIT images. Notably, after PID recovery tests for 75 h and 150 h, PID recovery behavior was not seen in EL and LIT images. It seems that the risk of high voltage stress becomes more severe. Furthermore, the dark areas in EL images appear at many places especially at the edges of the cell. Measurements of *J-V* characteristic curves and EQE responses were made at the micro-cracked region A marked by red-square in the EL images.

Figure 3a shows the relative losses of P_{max}, V_{oc}, FF, J_{sc}, and R_{sh} before and after PID stress and recovery processes. After a PID duration of 150 h, P_{max} degradation was 81% attributed to the losses of 48%, 58%, and 15% in V_{oc}, FF, and J_{sc}, respectively. Notably, the loss of electrical characteristics continued reducing even after the PID recovery process for 75 h and 150 h. The deterioration of P_{max}, V_{oc}, FF, and J_{sc} after the PID recovery process for 150 h was 87%, 57%, 61%, and 21%, respectively. Furthermore, EQE response was lost in the full wavelength range of 400 nm to 1,100 nm after a PID duration of 150 h, but it was not recovered after the PID recovery process for 75 h and 150 h, as shown in Figure 3b. The PID effect occurring at micro-cracked areas is due to PID shunting caused by the decoration of sodium (Na^+) ions on the across-section site of micro-cracks.[13] It is the crucial PID effect related to micro-cracks in p-type c-Si solar cells, which mainly causes the degradation of V_{oc} and FF. This effect is confirmed by the R_{sh} reduction of 99% measured at the micro-cracked region A after a PID duration of 150 h. However, R_{sh} is not recovered after the PID recovery process for 150 h. Also shown in Figure 3c, series resistance (R_s) increased 57% after PID duration of 150 h and even continued increasing 158% after PID recovery duration of 150 h. The elevated humidity within the package of the un-laminated solar module associated with acetic acid formation from the

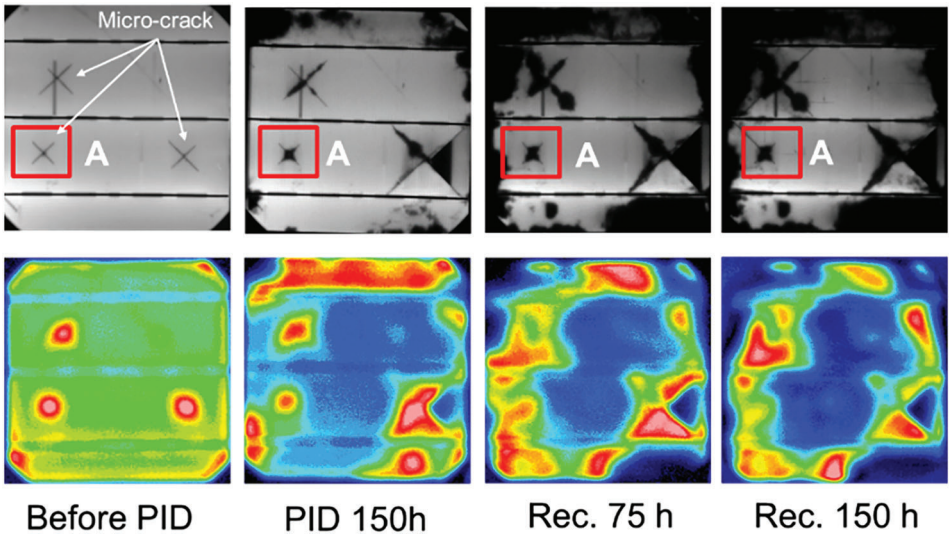

FIGURE 2 EL (the top row) and LIT (the bottom row) images of micro-cracked un-laminated solar modules before and after PID stress and recovery processes

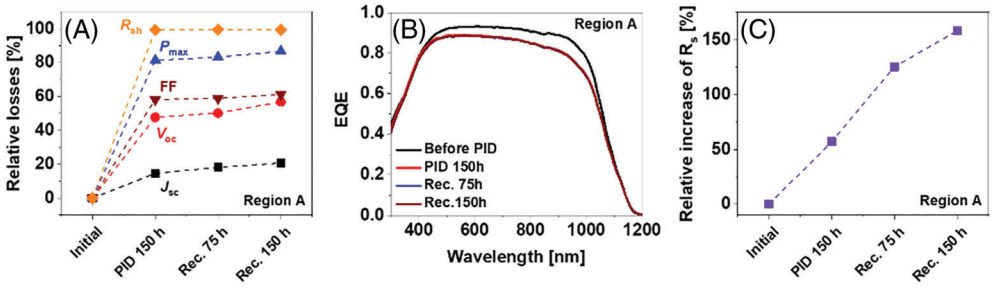

FIGURE 3 (A) Relative losses of electrical characteristics, (B) EQE responses, and (C) relative increase of series resistance (R_s) at the micro-cracked region A shown in Figure 2 before and after PID stress and recovery processes

encapsulation layer[19,20] under the high applied voltage bias causes electrolytic corrosion mainly at micro-cracked areas and the cell edge of the solar module.[4,21] Electrolytic corrosion causes the R_s increase, leading to the reduction of FF and J_{sc} at the micro-cracked region after both PID stress and recovery processes. This phenomenon also explains why dark areas appeared at the edges of the module in EL images. Furthermore, corrosion and dissolution of cell metallization due to electrochemical reactions at micro-cracked regions under the high voltage stress combined with damp-heat stress[22] are also considered as other causes for the performance degradation after the PID recovery process.

Likewise, we predicted that the elevated humidity at micro-cracked areas causes the increase of the surface conductivity on the cross-section site of micro-cracks. Under a high voltage bias combined with the high conductivity condition, Na^+ ions with high concentration could drift/diffuse into the deep inside of the micro-cracked areas. Therefore, it is difficult for a reverse voltage bias to push Na^+ ions out of micro-cracks during the PID recovery process. However, explicit evidence from further investigations should be essential to clarify this hypothesis. Thus, the PID recovery is a big problem for the PID-affected un-laminated solar module, especially, at micro-cracked areas and the edges. Although the PID recovery behavior could likely performed in un-laminated solar modules in the dry environment due to the low moisture penetration into the solar cell modules. The fact that solar cells usually operate in damp-heat environments, so the possibility of the PID recovery for un-laminated solar modules is still difficult. Therefore, the un-laminated solar module is convenient for microscopic analysis but adverse for PID recovery tests.

3.2 | The behavior of PID stress and recovery in laminated intact and micro-cracked solar modules

The comparison of PID stress and recovery behavior between laminated micro-cracked and intact solar modules was observed through EL images, as shown in Figure 4. The dark region in the micro-cracked solar cell was found mainly at the micro-cracked position and expended to nearby locations after a PID duration of 48 h and 72 h, respectively. Meanwhile, the dark region in the intact solar cell slightly changed mainly in the vicinity of the busbar after PID duration of 48 h and in the added corner area after 72 h. Thus, both Figures 2 and 4 showed that the PID effect also occurred at intact regions. This is

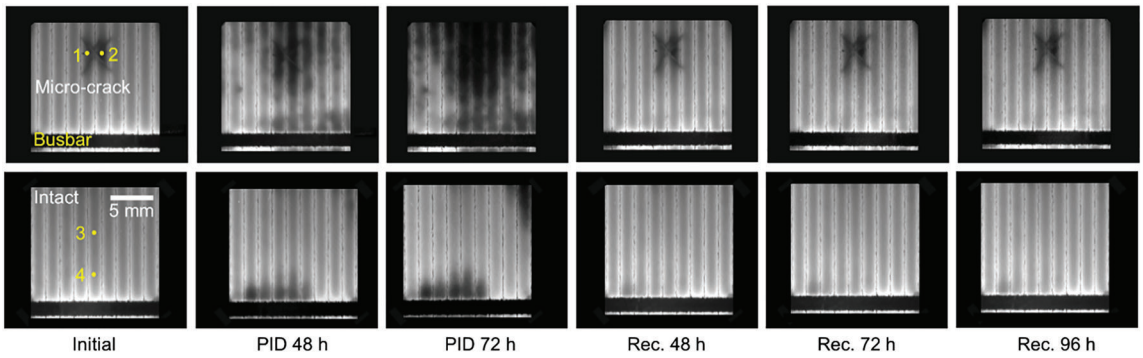

FIGURE 4 EL images of laminated intact and micro-cracked solar modules before and after PID stress and recovery processes. Note that points 1 and 2 (at the micro-cracked region) and points 3 and 4 (at the intact area) were marked for measurement of the effective carrier's lifetime

likely due to not only the PID shunting effect caused by the decoration of Na ions at local crystal defects such as stacking faults, and slight scratches in laminated solar modules, but also the additional electrolytic corrosion for un-laminated solar modules. However, it could be seen that PID behavior occurs more severely at the micro-cracked locations for laminated solar modules. The obtained results indicated that micro-cracks play a critical role in PID behavior, which is in good agreement with our previous work.[13] It is worth noting that the dark areas in the EL images of both laminated solar modules disappeared after the PID recovery process. Thus, PID recovery could be performed well in both laminated micro-cracked and intact modules.

Figure 5 shows one-sun illumination *J-V* curves of six intact and micro-cracked solar modules before and after PID stress and recovery processes. The noise of *J-V* curves is caused by the feed-back circuit to control the light intensity of our solar simulator set-up. It is observed that the deterioration level of electrical characteristics after the PID stress process in the micro-cracked modules was much more significant than that in the intact modules. The deterioration of electrical characteristics in the laminated micro-cracked modules, which was contributed by the losses of not only V_{oc}, FF, but also J_{sc}, is similar to the PID behavior at the micro-cracked areas of the before-mentioned un-laminated module. This result is also in good agreement with the achieved results of our previous work.[13] Notably, electrical characteristics in the PID-affected intact and micro-cracked modules were recovered well.

Electrical characteristics of solar cells, including P_{max}, V_{oc}, FF, J_{sc}, and R_{sh}, were averaged in three samples in each case for intact and micro-cracked modules. Figure 6 compares the averaged relative losses of P_{max}, V_{oc}, FF, J_{sc}, and R_{sh} between the intact modules and the micro-cracked modules before and after PID stress and recovery processes. In the micro-cracked modules, P_{max} severely deteriorates by 79% after the PID stress duration of 72 h, which was attributed to a V_{oc} loss of 45%, FF loss of 58%, and J_{sc} loss of 14%. All electrical characteristics regenerated significantly but incompletely by the PID recovery process of 72 h, which have relative losses of 19%, 3%, 17%, and 0.6% in P_{max}, V_{oc}, FF, and J_{sc}, respectively. The change of all electrical characteristics is negligible even after the PID recovery process up to 96 h, with relative losses of 19%, 4%, 16%, and 0.7% in P_{max},

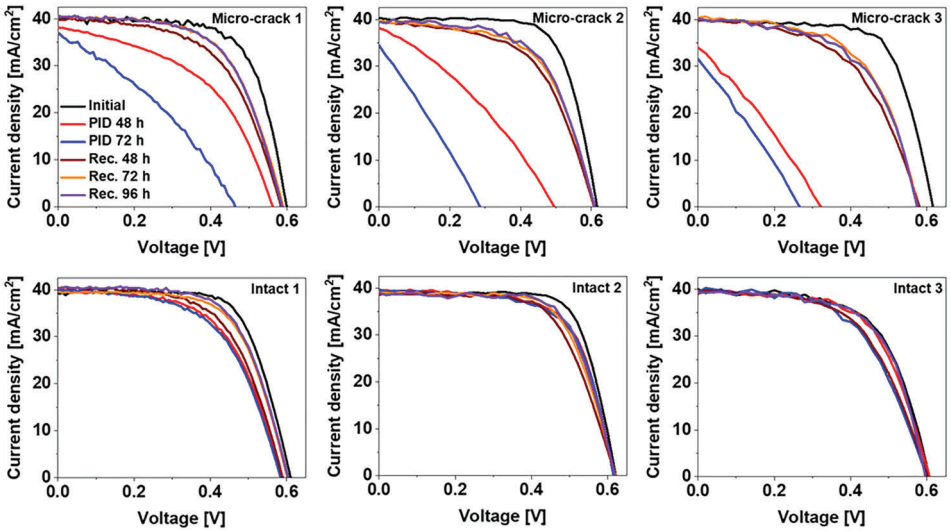

FIGURE 5 One-sun illumination J-V curves of the intact and micro-cracked solar modules before and after PID stress and recovery processes

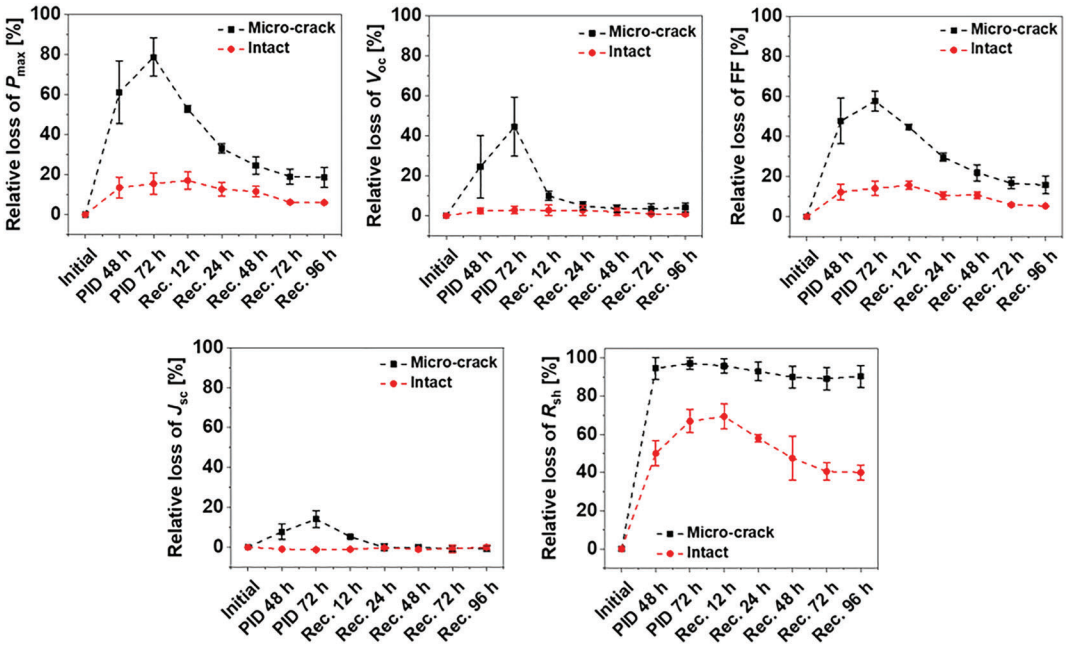

FIGURE 6 Comparison of relative losses *of* P_{max}, V_{oc}, *FF*, J_{sc}, and R_{sh} in tested solar modules micro-cracks before and after PID stress and recovery processes

V_{oc}, FF, and J_{sc}, respectively. Also shown in Figure 6, PID recovery behavior occurs quickly at an early stage. The performances gradually improve by the time and eventually saturates regardless of the increasing PID recovery duration. In the intact modules, P_{max} reduces by 15% contributed by degradations of 3% and 14% in V_{oc} and FF after PID stress duration of 72 h, respectively. The relative losses in P_{max}, V_{oc}, and FF are 6%, 0.8%, and 6% after the PID recovery duration of 72 h, and 6%, 0.7%, and 5% after the PID recovery duration of 96 h, respectively. Thus, the PID recovery was accomplished well but incompletely as well. After the PID stress process of 72 h, the R_{sh} relative loss of approximately 100% in the micro-cracked modules is more severe compared with the R_{sh} relative loss (67%) in the intact modules. After the PID recovery process of 72 h even 96 h, R_{sh} regenerated slightly (the R_{sh} relative loss of 90%) in the micro-cracked modules, while R_{sh} in the intact modules was recovered more significantly (the R_{sh} relative loss of 44%). This is because the decoration of Na ions in micro-cracks is more severe than that in other crystal defects (dominant stacking faults), so it is more difficult for Na ions to diffuse out of micro-cracks compared with other crystal defects. However, the incomplete regeneration of R_{sh} in micro-cracked even intact modules due to the PID recovery process is good agreement with the literature.[15] This observation revealed that the PID-affected level in the micro-cracked solar modules is more severe than that in the intact ones. Possibly, only a specific portion of Na^+ ions was diffused out of shunted regions such as stacking faults and micro-cracks after the PID recovery. Therefore, the R_{sh} regeneration in the intact and micro-cracked modules after the PID recovery is incomplete regardless of increasing the PID recovery duration, leading to their non-full PID recovery behavior.

Furthermore, the comparison of EQE responses before and after PID stress and recovery processes between intact module no. 1 (intact 1) and micro-cracked module no.1 (micro-crack 1) was indicated in Figure 7. It is noted that the EQE response in the micro-cracked area of the laminated micro-cracked solar module after PID stress of 72 h is noisy because of the EQE scaling error when measuring severely shunted cells, as demonstrated in the literature.[23] It could be seen that the EQE response in the intact module shows no change before and after PID stress and recovery processes. This observation indicates that only the electrical shunt path influences the performance degradation due to PID in p-type c-Si solar cells without micro-cracks, as investigated in works.[24–26] It is also important to mention that the EQE response in the micro-cracked modules dropped significantly after the PID stress process but was almost completely recovered. The loss of the EQE response after PID stress revealed that micro-cracked areas decorated by Na ions act as recombination centers. Possibly, the EQE regeneration caused by the PID recovery process is due to the Na-ion out-diffusion from micro-cracked areas under applied high reverse voltage. The decrease and increase of the EQE response cause degradation and regeneration of V_{oc} and J_{sc} after PID stress and recovery processes, respectively.

The μ-PCD signal and the τ_{eff} value were measured at two points (1 and 2) for the micro-cracked region of each micro-cracked module and at two points (3 and 4) for the intact region of each intact module. Herein, four points from 1 to 4 were marked in Figure 4. Figure 8a,b shows the μ-PCD signal for the intact module no. 1 (intact 1) and the micro-cracked module no. 1 (micro-crack 1), respectively. It is observed that the μ-PCD signals, including rapid and slow time

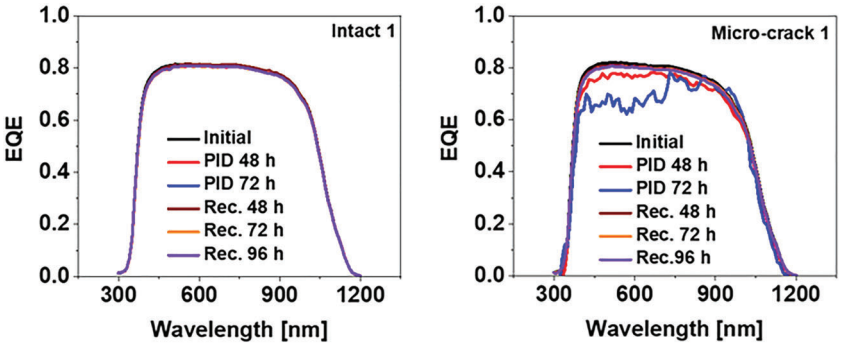

FIGURE 7 EQE response behavior of intact and micro-cracked solar modules before and after PID stress and recovery processes

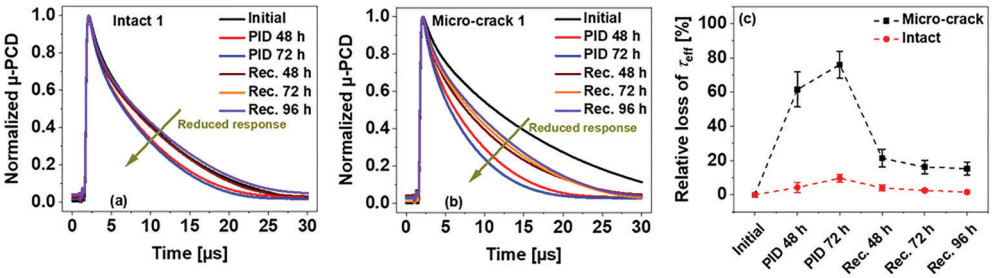

FIGURE 8 Normalized μ-PCD responses of the intact and micro-cracked solar modules (a, b) and τ_{eff} relative losses at the intact and micro-cracked areas (c) before and after the PID stress and recovery processes

constant decay components, in both cases, presented faster decay profile after the PID stress process. However, the reduction level of the μ-PCD signal for the micro-cracked module is much more significant than that for the intact module after the PID stress process. In addition, the μ-PCD signal due to the PID recovery process for the intact module was almost completely regenerated while that for the micro-cracked module was retrieved incompletely.

In each case, the τ_{eff} values were averaged in three modules and listed in Table 1. The average τ_{eff} relative losses at the intact and micro-cracked positions after the PID stress and recovery processes were presented in Figure 8c. The average τ_{eff} reduction in the intact modules is suspected to be influenced by the Na-decorated stacking faults, which act as shunting defects across the p-n junction. However, the τ_{eff} loss in the micro-cracked modules is thought to be due to both shunting defects and additional recombination centers at the micro-cracked areas. After the PID recovery process, the τ_{eff} value in both cases was regenerated effectively but did not reach the original value, in particular, for the micro-cracked modules. The out-diffusion of Na^+ ions from micro-cracked areas, resulting in the suppression of carrier recombination, could be considered a possibility, which regenerates the τ_{eff} value. However, the minimizing of carrier recombination centers is not efficient enough to fully recover the τ_{eff} value at micro-cracked areas. It could be seen the τ_{eff} degradation and regeneration behavior at the micro-cracked positions is a good correlation with the solar module performance behavior of the micro-cracked module before and after the PID stress and recovery processes. It is supposed that the μ-PCD response and the τ_{eff} value act as indicators to examine the electrical characteristics of solar modules before and after PID stress and recovery processes for solar modules with and without micro-cracks.

TABLE 1 Average τ_{eff} values at the intact and micro-cracked positions before and after the PID stress and recovery processes

	Averaged effective carrier's lifetime τ_{eff} (μs)	
	At the intact position	At the micro-cracked position
Initial	11.53 ± 0.47	12.10 ± 0.19
PID 48 h	11.04 ± 0.62	4.67 ± 1.27
PID 72 h	10.42 ± 0.47	2.91 ± 0.97
Rec. 48 h	11.07 ± 0.47	9.52 ± 0.62
Rec. 72 h	11.24 ± 0.43	10.15 ± 0.49
Rec. 96 h	11.35 ± 0.37	10.26 ± 0.46

3.3 | The degradation and regeneration behavior of laminated micro-cracked modules due to the PID effect after PID stress/recovery cycles

Biasing high negative potential will result in the performance loss, whereas applying high positive potential will regenerate the module performances partially. The PID stress/recovery cycles are an essential first step to examine the cyclic PID behavior of the solar modules and to choose the best scenario for degradation and recovery. Three principle rate scenarios for solar modules after the PID stress/recovery cycles could be conducted by Pingel.[27] Firstly, the regeneration

rate of the PID recovery process is slower than the degradation rate of the PID stress process; that is, the relative loss of electrical characteristics due to the PID stress process tends to increase after cyclic PID stress/recovery tests. In this scenario, the solar modules are susceptible to PID. Secondly, the regeneration rate of the PID recovery process is similar to the degradation rate of the PID stress process; that is, the relative loss of electrical characteristics due to the PID stress process tends to be stable after cyclic PID stress/recovery tests. Herein, the PID effect is stable over PID stress/recovery cycles. Thirdly, the regeneration rate of the PID recovery process is faster than the degradation rate of the PID stress process; that is, the relative loss of electrical characteristics due to the PID stress process tends to decrease after cyclic PID stress/recovery tests. In this case, the performance of the PID-affected solar module will increase over time, which is the best scenario for the solar modules to control the PID effect.

Figure 9a–d shows the degradation and regeneration behavior due to the PID effect for the micro-cracked solar modules over 11 PID stress/recovery cycles. The values of electrical characteristics were averaged in three modules. Herein, the relative losses of the average electrical characteristics were calculated by their initial values (before PID stress). Although the deterioration caused by the PID effect related to micro-cracks is severe, the relative losses of P_{max}, V_{oc}, FF, and J_{sc} due to the PID stress process tend to decrease gradually and stable after stress/recovery cycles. The stable relative losses of P_{max}, V_{oc}, FF, and J_{sc} due to the PID stress process after nine PID stress/recovery cycles are 20%, 6%, 19%, and 0.4%, respectively. The above findings are likely because of the following reason. With an appropriate PID recovery duration, the penetration of Na ions into the cell active layer and then crystal defects (stacking faults, micro-cracks etc.) due to the PID test process is reduced gradually after each test cycle. This eliminates the PID effect gradually after each test cycle. However, its detailed mechanism needs further investigations.

Meanwhile, the regeneration of P_{max}, V_{oc}, FF, and J_{sc} due to the PID recovery process is incomplete but relatively stable after each stress/recovery cycle. In addition, the stable relative losses of P_{max}, V_{oc}, FF, and J_{sc} due to the PID recovery process after nine PID stress/recovery cycles are 15%, 2%, 12%, and 2%, respectively. In this work, the PID stress and recovery processes have a similar duration; the performance loss of tested solar modules tends to subside (the first phase) and then stable (the second phase) after the PID stress/recovery cycles. The first phase is in good agreement with the third scenario mentioned above. The second phase just occurs after a sufficient number of the PID stress/recovery cycles. The result in this work is supposed more reasonable and realistic. It is evidence to believe that the performance degradation of intact or micro-cracked solar modules due to PID could be controlled after PID stress/recovery cycles. It is noted that this scenario was activated by the electrical recovery method but not triggered by temperature even for intact modules.[28]

It was observed that the relative losses of P_{max}, V_{oc}, FF, and J_{sc} due to the PID stress process decrease with increasing the number of PID stress/recovery cycles. However, the correlation between the relative losses of P_{max}, V_{oc}, FF, and J_{sc} due to the PID stress process and the number of PID stress/recovery cycles has not been revealed. In this work, the authors investigated the correlation based on an exponential decreasing model:

$$y = A_0 e^{(-x/\tau)} + y_0 \quad (3)$$

where A_0, x, y, and τ parameters are amplitude, cycle number, the relative loss of electrical characteristics, and exponential time constant,

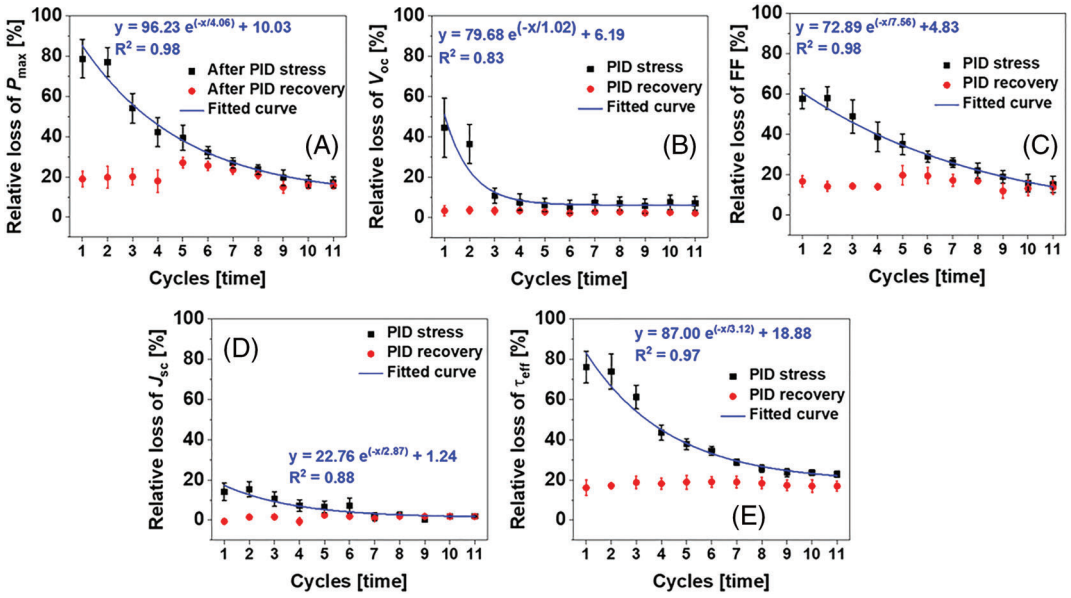

FIGURE 9 The degradation and regeneration behavior of electrical characteristics for the micro-cracked solar module over 11 PID stress and recovery cycles

TABLE 2 Fitted parameters for the exponential decreasing model of relative losses

$y = A_0e^{(-x/\tau)} + y_0$					
Relative loss (%)	**A_0 (%)**	**τ**	**y_0 (%)**	**Decreasing rate ($\lambda = 1/\tau$)**	**Fitted coefficient (R^2)**
P_{max}	96	4.06	10	0.25	0.98
V_{oc}	80	1.02	6	0.98	0.83
FF	73	7.56	5	0.13	0.98
J_{sc}	23	2.87	1	0.35	0.88

respectively. The fitted curves of the relative losses of P_{max}, V_{oc}, FF, and J_{sc} due to the PID stress process versus the number of the PID stress/recovery cycles, as illustrated in the fitted curves of Figure 9. As listed in Table 2, although the fitted coefficients (R^2) of determination in the cases of V_{oc} and J_{sc} are lower than that in the cases of P_{max}, FF, generally, R^2 for each case is highly correlated.

This finding verifies that the relationship of the relative losses of P_{max}, V_{oc}, FF, and J_{sc} due to the PID stress process and the number of the PID stress/recovery cycles actively complies with an exponentially decreasing function. According to the exponential model, the relative losses of P_{max}, V_{oc}, FF, and J_{sc} due to the PID stress process could reach to the critical points of 10%, 6%, 5%, and 1% after a certain number of the PID stress/recovery cycles, respectively. The critical point (10%) of the P_{max} relative losses coincides with the experimental result in the literature,[27] which reported power regeneration of over 90% after PID stress/recovery cycles in a period of several years. Thus, the cyclic PID test could prevent solar modules from the PID effect significantly. Remarkably, the decreasing rate (0.98) of the V_{oc} relative loss is the highest; that is, the V_{oc} regeneration rate is the fastest. Furthermore, the relative loss of the τ_{eff} value versus PID stress/recovery cycles, as shown in Figure 9e, was also investigated by the exponential model. A strong exponential agreement between the relative loss of the τ_{eff} value and PID stress/recovery cycles could be approximated by the fitted function $y = 87e^{(-x/3.12)} + 18.88$ with the highly fitted coefficient of 0.97. This confirmed that the μ-PCD response and the τ_{eff} value act as indicators to examine the electrical characteristics of solar modules.

Whether the cyclic PID test method is a feasible solution for minimizing the PID effect or not, it depends on relevant factors such as PID duration, PID recovery duration, the number of PID stress/recovery cycles, temperature, humidity, etc. Further investigations of the cyclic PID test will realize a more stable performance, even receiving PID condition, while this work presented a critical step towards this goal.

4 | CONCLUSIONS

This work demonstrated that the PID shunting path due to the decoration of Na^+ ions at the micro-cracked areas acts as the primary PID mechanism causing the losses of V_{oc} and FF for p-type c-Si solar modules. The micro-cracked regions are also supposed as the additional recombination centers, leading to the reduction of J_{sc} and V_{oc} of solar modules after PID stresses. The PID effect in the micro-cracked solar modules is more severe than the intact solar modules. Furthermore, the PID recovery possibility is difficult to achieve by biasing a high reverse voltage for un-laminated solar cells regardless of with or without micro-cracks, even the more significant degradation due to the high voltage stress. However, the PID recovery has been made significantly but incompletely for both laminated intact and micro-cracked solar cells by the same PID recovery method above. The average loss of P_{max} is about 79% after a PID stress duration of 72 h, but it is 19% and 19% after a PID recovery duration of 72 h and 96 h, respectively. The authors supposed that the PID recovery behavior occurs quickly at an early stage, then subsides after time and eventually saturates regardless of increasing PID recovery duration. The incomplete recovery behavior of PID-affected solar cells is attributed to the incomplete recovery of R_{sh} and FF. The degradation and regeneration of the τ_{eff} value are a function of the PID stress and recovery processes. The μ-PCD response also plays a critical role in indicating the PID effect due to micro-cracks of solar cells. Finally, this work also performed the cyclic PID tests for 11 cycles with the same stress/recovery duration of 72 h. The achieved results showed the decreasing tendency of the loss of electrical characteristics due to the PID stress process after PID degradation/recovery cycles. Notably, the correlation between the relative losses of P_{max}, V_{oc}, FF, and J_{sc} due to the PID stress process and the number of the PID stress/recovery cycles was modeled by the exponential decreasing function. This model revealed that the cyclic PID test method could maintain P_{max} of solar cells up to 90% (as shown in Table 2) in solar cells after a long time of several years. Thus, the cyclic PID test method can suppress/reduce PID behavior effectively. Therefore, we suggest that the cyclic PID test with suitable conditions might be an easy and cost-effective way to control the PID effect.

ORCID

Dong C. Nguyen https://orcid.org/0000-0002-9948-2091
Yasuaki Ishikawa https://orcid.org/0000-0003-4613-6117

REFERENCES

1. Pingel S, Frank O, Winkler M, *et al*. Potential induced degradation of solar cells and panels. *35th IEEE Photovoltaic Specialists Conference*. 2010:2817–2822.
2. Berghold J, Frank O, Hoehne H, Pingel S, Richardson S, Winkler M. Potential induced degradation of solar cells and panels. *25th European Photovoltaic Solar Energy Conference and Exhibition/5th World Conference on Photovoltaic Energy Conversion* 2010:3753–3759.
3. Schütze M, Junghänel M, Koentopp MB, *et al*. Laboratory study of potential induced degradation of silicon photovoltaic modules. *37th IEEE Photovoltaic Specialists Conference*. 2011:821–826.
4. Hacke P, Kempe M, Terwilliger K, *et al*. Characterization of multicrystalline silicon modules with system bias voltage applied in damp

heat. *25th European Photovoltaic Solar Energy Conference and Exhibition/5th World Conference on Photovoltaic Energy Conversion*. 2010:3760–3765.
5. Hara K, Jonai S, Masuda A. Potential-induced degradation in photovoltaic modules based on n-type single crystalline Si solar cells. *Sol Energy Mater Sol Cells*. 2015;140:361-365.
6. Yamaguchi S, Masuda A, Ohdaira K. Progression of rapid potential-induced degradation of n-type single-crystalline silicon photovoltaic modules. *Appl Phys Express*. 2016;9(11):112301-112301.
7. Swanson R, Cudzinovic M, Deceuster D, *et al*. The surface polarization effect in high- efficiency silicon solar cells. *15th International Photovoltaic Science & Engineering Conference* 2005:410–411.
8. Ziebarth B, Mrovec M, Elsässer C, Gumbsch P. Potential-induced degradation in solar cells: electronic structure and diffusion mechanism of sodium in stacking faults of silicon. *J Appl Phys*. 2014;116(9):1-7, 093510.
9. Nguyen DC, Ishikawa Y, Jonai S, Nakamura K, Masuda A, Uraoka Y. Elucidating the mechanism of potential induced degradation delay effect by ultraviolet light irradiation for p-type crystalline silicon solar cells. *Sol Energy*. 2020;199:55-62.
10. Israil M, Anwar SA, Abdullah MZ. Automatic detection of micro-crack in solar wafers and cells: a review. *Trans Inst Meas Control*. 2013;35 (5):606-618.
11. Käsewieter J, Haase F, Larrodé MH, Köntges M. Cracks in solar cell metallization leading to module power loss under mechanical loads. *Energy Procedia*. 2014;55:469-477.
12. Köntges M, Kunze I, Kajari-Schröder S, Breitenmoser X, Bjørneklett B. The risk of power loss in crystalline silicon based photovoltaic modules due to micro-cracks. *Sol Energy Mater Sol Cells*. 2011;95(4):1131-1137.
13. Dong NC, Islam MA, Ishikawa Y, Uraoka Y. The influence of sodium ions decorated micro-cracks on the evolution of potential induced degradation in p-type crystalline silicon solar cells. *Sol Energy*. 2018; 174:1-6.
14. Lausch D, Naumann V, Breitenstein O, et al. Potential-induced degradation (PID): introduction of a novel test approach and explanation of increased depletion region recombination. *IEEE J Photovoltaics*. 2014; 4(3):834-840.
15. Lausch D, Naumann V, Graff A, et al. Sodium outdiffusion from stacking faults as root cause for the recovery process of potential-induced degradation (PID). *Energy Procedia*. 2014;55:486-493.
16. Ma L, Xu L, Zhang K, *et al*. The measurement of series and shunt resistances of the silicon solar cell based on LabVIEW, *2011 International Conference on Electrical and Control Engineering* 2011: 2711–2714.
17. Ishibashi K, Kimura Y, Niwano M. An extensively valid and stable method for derivation of all parameters of a solar cell from a single current-voltage characteristic. *J Appl Phys*. 2008;103(9):1-6, 094507.
18. Islam MA, Nguyen DC, Ishikawa Y. Effective minority carrier lifetime as an indicator for potential-induced degradation in p-type single-crystalline silicon photovoltaic modules. *Jpn J Appl Phys*. 2019;58(10): 106507-106507.
19. Whitfield K, Salomon A, Yang S, Suez I. Damp heat versus field reliability for crystalline silicon. *38th IEEE Photovoltaic Specialists Conference* 2012:1864–1870.
20. Czanderna AW, Pern FJ. Encapsulation of PV modules using ethylene vinyl acetate copolymer as a pottant: a critical review. *Sol Energy Mater Sol Cells*. 1996;43(2):101-181.
21. Mon G, Wen L, Ross RG, Adent D. Effects of temperature and moisture on module leakage current. *18th IEEE Photovoltaic Specialists Conference* 1985:1179–1185.
22. Kempe MD, Jorgensen GJ, Terwilliger KM, McMahon TJ, Kennedy CE, Borek TT. Acetic acid production and glass transition concerns with ethylene-vinyl acetate used in photovoltaic devices. *Sol Energy Mater Sol Cells*. 2007;91(4):315-329.
23. Oh J, Bowden S, TamizhMani G. Potential-induced degradation (PID): incomplete recovery of shunt resistance and quantum efficiency losses. *IEEE J Photovoltaics*. 2015;5(6):1540-1548.
24. Hacke P, Terwilliger K, Smith R, *et al*. System voltage potential-induced degradation mechanisms in PV modules and methods for test. *37th IEEE Photovoltaic Specialists Conference*. 2011:814–000820.
25. Naumann V, Hagendorf C, Grosser S, Werner M, Bagdahn J. Micro structural root cause analysis of potential induced degradation in c-Si solar cells. *Energy Procedia*. 2012;27:1-6.
26. Naumann V, Lausch D, Großer S, et al. Microstructural analysis of crystal defects leading to potential-induced degradation (PID) of Si solar cells. *Energy Procedia*. 2013;33:76-83.
27. Pingel S. Recovery methods for modules affected by potential induced degradation (PID), *27th European Photovoltaic Solar Energy Conference* 2012: 3379–3383.
28. Nagel H, Pfeiffer R, Raykov A, Wangemann K. Lifetime warranty testing of crystalline silicon modules for potential-induced degradation. *27th European Photovoltaic Solar Energy Conference and Exhibition* 2012:3163–3166.

How to cite this article: Nguyen DC, Ishikawa Y, Uraoka Y. Recover possibilities of potential induced degradation caused by the micro-cracked locations in p-type crystalline silicon solar cells. *Prog Photovolt Res Appl*. 2020;1–10. https://doi.org/10.1002/pip.3383